Eur. Phys. J. A **31**, 15–22 (2007)
DOI 10.1140/epja/i2006-10150-5

THE EUROPEAN PHYSICAL JOURNAL A

Regular Article – Nuclear Structure and Reactions

# Do we understand the electric quadrupole strength distributions in magic nuclei?

J. Enders[a], O. Karg[b], P. von Neumann-Cosel, and V.Yu. Ponomarev[c]

Institut für Kernphysik, Technische Universität Darmstadt, Schlossgartenstraße 9, D-64289 Darmstadt, Germany

Received: 31 August 2006 / Revised: 27 November 2006
Published online: 9 January 2007 – 
Communicated by R. Krücken

**Abstract.** A comparison between the electric quadrupole ($E2$) strength distributions in $^{40,48}$Ca with new results from $^{52}$Cr is presented. The deduced $E2$ strength distributions and the exhaustion of the isoscalar energy-weighted $E2$ sum rule are very different. Microscopic approaches fail to reproduce these differences. A survey of the available data shows that the exhaustion of the energy-weighted isoscalar $E2$ sum rule in doubly magic nuclei below the isoscalar giant quadrupole resonance is typically more than two times larger than in semi-magic nuclei. On the other hand, the $E2$ strength in this energy region exhausts about 50% of the total $E2$ strength, independent from shell closures.

**PACS.** 21.10.-k Properties of nuclei; nuclear energy levels – 21.60.-n Nuclear structure models and methods – 25.20.Dc Photon absorption and scattering

## 1 Introduction

The occurrence of low-lying electric quadrupole ($E2$) excitations is a key finding of the structure of atomic nuclei. In the overwhelming majority of nuclei with even proton and neutron number one finds a $2^+_1$ state as the first excited state which often —especially in non-magic nuclei— exhibits collective features and can be interpreted as due to a quadrupole vibration or a collective rotation of the nucleus. A measure of the collectivity is given by the $E2$ strength for the excitation of the $2^+_1$ state from the ground state (g. s.). A relation between these excitation strengths, which typically exceed single-particle estimates, and the excitation energies of the $2^+_1$ states was first established by Grodzins [1]. From these quantities, one can derive deformation parameters for the nuclei and lifetimes of the $2^+_1$ states as well as compare the measured values with nearly model-independent estimates such as the energy-weighted sum rule (EWSR). For an overview, see the latest compilation by Raman, Nestor, and Tikkanen [2]. In magic nuclei, one typically finds high excitation energies of the $2^+_1$ state and low values of $B(E2; 0^+_1 \rightarrow 2^+_1)$ as a consequence of large shell gaps, a fact that, to a lesser extent, still holds for semi-magic nuclei.

At high excitation energies the $E2$ strength is dominated by the isoscalar giant quadrupole resonance (ISGQR) which arises from a coherent superposition of many one-particle–one-hole excitations across two major shells. Its excitation energy varies smoothly with the mass number [3], and shell effects play only a role in the proposed damping mechanisms [4]. The ISGQR is expected to dominate, due to its high excitation energy, the EWSR for isoscalar $E2$ excitations which we write following ref. [2]:

$$\begin{aligned} S(E2) &= \sum E_{\mathrm{x},i} \cdot B_i(E2) \uparrow \\ &= 30 \left(\frac{Z}{A}\right)^2 \frac{(\hbar c)^2}{8\pi\, m_p c^2}\, A\, e^2\, R_0^2 \\ &= 71.34 \frac{Z^2}{A^{1/3}}\, e^2 \mathrm{fm}^4\, \mathrm{MeV}. \end{aligned} \tag{1}$$

Here, the charge and mass number of a nucleus are given by $Z$ and $A$, respectively, the nuclear radius $R_0 = 1.2\, A^{1/3}$ fm is related to the single-particle mean-square radius by $(3/5) \cdot R_0^2$, and $m_p$ is the proton mass. Since Grodzins' rule [1] suggests that the product $E_{\mathrm{x}}(2^+_1) \cdot B(E2; 0^+_1 \rightarrow 2^+_1)$ is approximately constant (although this does not hold too well for magic nuclei), one can say that the excitation of the $2^+_1$ state roughly exhausts a constant fraction of the isoscalar EWSR in nuclei of the same mass region [2].

[a] e-mail: enders@ikp.tu-darmstadt.de
[b] *Present address*: Fachgebiet Elektronische Materialeigenschaften, Technische Universität Darmstadt, D-64287 Darmstadt, Germany.
[c] *Permanent address*: Bogoliubov Laboratory of Theoretical Physics, Joint Institute for Nuclear Research, 141980 Dubna, Russia.

Recent photon scattering experiments [5,6] have detected significant $E2$ strength in the doubly magic nuclei $^{40,48}$Ca well below the ISGQR. This strength is not concentrated in the $2^+_1$ state, but distributed over several states up to 10 MeV. Therefore, the EWSR is exhausted significantly by the low-lying $E2$ strength, as was already discussed in ref. [6]. For $^{40}$Ca, the exhaustion of the sum rule amounts to 25%, for $^{48}$Ca even to about 40%, *i.e.*, a large fraction of the total $E2$ strength resides below the ISGQR.

In order to see if this finding is peculiar to the double shell closure, we have performed a nuclear resonance fluorescence experiment on the semi-magic $N = 28$ nucleus $^{52}$Cr comparable to the work of Hartmann *et al.* [5,6]. In a previous study of $^{52}$Cr [7], indications were found for a couple of $2^+$ states around 6 MeV excitation energy, and the new experiment aimed at a validation of the $2^+$ assignment of these states and a search for more $E2$ strength up to about 10 MeV with increased sensitivity. After presenting the setup, the results, and the detection threshold of the photon scattering experiment, we discuss the results of model calculations on the $E2$ strength distributions in $^{52}$Cr and $^{48}$Ca in sect. 4. Section 5 contains a systematic analysis of $E2$ strength distributions for several magic and semi-magic nuclei.

## 2 Nuclear resonance fluorescence on $^{52}$Cr

### 2.1 Experiment

The experiment was carried out at the low-energy bremsstrahlung setup [8] of the superconducting Darmstadt electron linear accelerator S-DALINAC [9] using two high-purity germanium gamma-ray detectors with an efficiency of 100% relative to a $3'' \times 3''$ NaI(Tl) detector at 1.33 MeV. The two detectors were placed at 90° and 130° relative to the photon beam direction, close to extremal values of the angular distributions of the quadrupole excitations. Both detectors were actively shielded by surrounding them with BGO scintillators. The $(\gamma, \gamma')$ reaction was studied at two endpoint energies of the bremsstrahlung, 8.0(1) MeV and 9.9(1) MeV, with average electron beam currents of 42 $\mu$A and 45 $\mu$A, respectively. For the experiment with 9.9 MeV endpoint energy, a 996.4(5) mg enriched (99.8%) $^{52}$Cr target was used, sandwiched between natural boron disks with a total mass of 1004.1(5) mg; data were taken for 62 hours. The 8 MeV endpoint energy experiment made use of a natural $^{52}$Cr target ($^{52}$Cr abundance 83.8%) with a mass of 2954(1) mg combined with the above-mentioned boron disks; the data acquisition time was 23 hours.

### 2.2 Results

Figure 1(a) shows the spectrum between 4 and 10 MeV taken with the detector placed at 90° with respect to the incident beam from the measurement with 9.9 MeV endpoint energy. At this angle, a local maximum of the angular distribution occurs for transitions from the g. s. into a $2^+$ level and back to the $0^+$ g. s. The angular-distribution ratio between the 90° detector and the 130° detector serves for the identification of the angular momentum of the excited state; it is plotted for all transitions into the g. s. in fig. 1(b). The transitions from $^{11}$B are nearly isotropic, as expected. From fig. 1(b) it is evident that, above 4 MeV, no $E2$ excitations from the g. s. have been observed, in contrast to the tentative assignments in ref. [7].

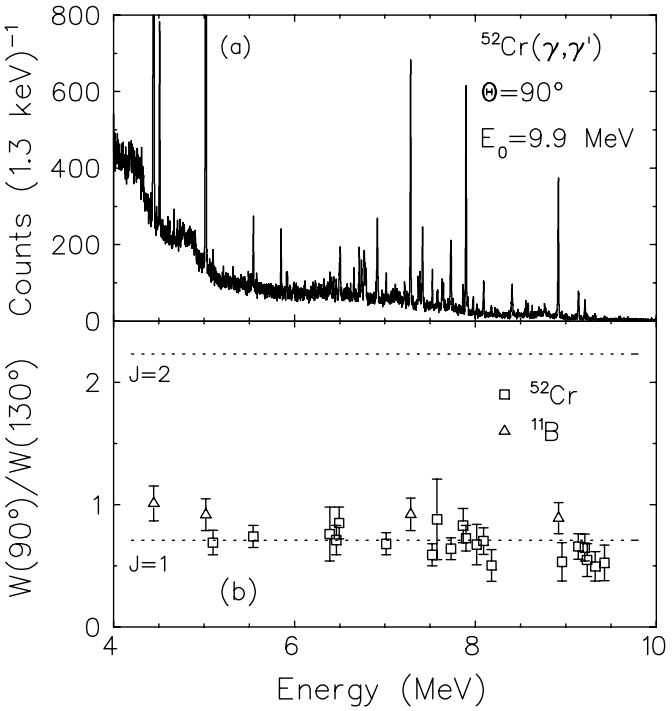


**Fig. 1.** (a) Nuclear resonance fluorescence spectrum of the $^{52}$Cr target at an endpoint energy of 9.9(1) MeV measured with the germanium detector placed at 90° with respect to the incident beam for the energy interval between 4 and 10 MeV. (b) Angular-distribution ratio $W(90°)/W(130°)$ for transitions in $^{52}$Cr (squares) and in $^{11}$B (triangles) used for the photon flux determination. The latter are expected to be nearly isotropic, while dipole excitations in $^{52}$Cr have ratios around 0.7 (dotted line) and quadrupole excitations should have a ratio of about 2.2 (dotted line).

The well-known transitions from $^{11}$B [10] served for a combined efficiency and photon flux calibration aided by simulations of the photon flux and detector efficiency with the code GEANT3 [11] using the empirical corrections suggested in ref. [12]. The strengths of the excitation of the $2^+$ states at 1434 keV, 2965 keV, and 3162 keV could not be determined from the present experiment as they were either not observed or strongly fed by the decay of higher-lying states. We have taken these $B(E2)$ values from the literature [13]. The $E2$ strength of the 3772 keV state was found to be 71(8) $e^2$fm$^4$, in good agreement with the previous measurement of ref. [7] which reported 76(11) $e^2$fm$^4$. Table 1 lists the measured $E2$ excitations in $^{52}$Cr with their strengths. For most of the transitions observed in ref. [7] no information about the angular momentum of the excited states is available. The present experiment

**Table 1.** Excitation energies and strengths of $2^+$ states in $^{52}$Cr.

| $E_x$ (keV) | $B(E2)\uparrow$ ($e^2$fm$^4$) | Ref. |
|---|---|---|
| 1434 | 660(30) | [2] |
| 2965 | 0.3(2) | [13] |
| 3162 | 12.4(23) | [13] |
| 3772 | 71(8) | this work |
| Sum | 744(41) | |

assigns dipole character to all of them above the 3772 keV state. A complete analysis of the dipole excitations measured will be given elsewhere [14]. Especially the states at 6137 keV and 6494 keV, to which formerly $J^\pi = 2^+$ was attributed [7,13], have turned out to be due to background and due to a dipole excitation, respectively. The $2^+$ assignment of the latter state was based on a previously measured angular distribution in proton scattering [15]. The summed $E2$ strength in $^{52}$Cr up to 9.9 MeV is 744(41) $e^2$fm$^4$ which is nearly twice as much as in $^{48}$Ca. However, the exhaustion of the isoscalar EWSR amounts to 11.6(8)% only, compared to more than 40% in $^{48}$Ca.

## 3 Detection threshold and level densities

One may wonder whether the striking difference between the exhaustions of the EWSR in $^{48}$Ca and its isotone $^{52}$Cr could be explained by the experimental conditions. At energies between 7 and 9 MeV, the present experiment would detect all $E2$ excitations with $B(E2)\uparrow \geq\sim 5\ e^2$fm$^4$ (depending on excitation energy) under the assumption that the excited state decays into the g. s. only. However, a higher level density —as is expected in a semi-magic nucleus compared with the doubly magic case— would i) distribute the complete strength to more states and ii) might cause significant decay branches into a larger number of low-lying states.

Microscopic model predictions [16,17] indeed expect the level density of $2^+$ states in $^{52}$Cr to be about a factor of 3 to 5 higher than in $^{48}$Ca, namely about 30 states per MeV at 8 MeV excitation energy (for $^{48}$Ca, 9 MeV$^{-1}$ are predicted, much more than observed experimentally). The microscopic model predicts somewhat higher level densities compared to phenomenological analyses such as the constant-temperature model [18] or a back-shifted Fermi-gas model [18,19], but the general trend is comparable. (For a comparison, we have used the latest compilation of von Egidy and Bucurescu [20] for the nuclei $^{40}$Ca and $^{50}$Ti as no data for $^{48}$Ca and $^{52}$Cr are given. Here, the level density in the semi-magic nucleus is larger by a factor of 3 to 5, too.) Higher level densities can have a tremendous impact on the strength distribution. An example might be the fragmentation of the spin-$M1$ strength in the $N = 28$ isotones studied in electron scattering [21]. This behavior is well described by recent theoretical approaches [22, 23] that may provide guidance in rating the importance of the level-density effect on the fragmentation of the $E2$ strength.

Weak unobserved decay branches into low-lying states could additionally raise the effective detection threshold because in nuclear resonance fluorescence the measured cross-section is proportional to $\Gamma_0^2/\Gamma$ with $\Gamma_0$ and $\Gamma$ being the partial decay width into the g. s. and the total decay width, respectively. Comparing the extracted cross-sections for dipole excitations in $^{52}$Cr from the photon scattering reaction [14,24,25] with the transition strength from an electron scattering experiment [21] measuring $\Gamma_0$, one indeed finds evidence for branching ratios decreasing from unity to values around 30%. Therefore, one cannot exclude that some strength might have escaped detection for $E2$ transitions, as well. Only four to five states located around 8 MeV with branching ratios into the g. s. of approximately 30% and a cross-section compatible with the detection threshold could therefore possibly carry enough strength to double the exhaustion of the $E2$ EWSR in $^{52}$Cr at low energies. However, as we will discuss in the following two sections, this is neither expected from microscopic models nor from systematics.

## 4 Theoretical analysis

### 4.1 $^{52}$Cr

In the following, we try to shed light on the experimental findings looking at microscopic model calculations. The detected $E2$ strength distribution in $^{52}$Cr, which is depicted in the top panel (a) of fig. 2 together with the experimental detection threshold between 5 and 9 MeV for states with 100% decay branch into the g. s., is accounted for by $fp$-shell ($0\hbar\omega$) shell model calculations. Using the FPD6 interaction [26] as an example with the code OXBASH [27] regarding excitations from the $0f_{7/2}$ orbital into $1p_{3/2}$, $0f_{5/2}$, and $1p_{1/2}$, one finds a strong transition to the $2_1^+$ state. Transitions to a few excited states around 8 MeV are also predicted with cross-sections slightly above the experimental detection limits (if these states would decay to the g. s. almost exclusively). This is shown in fig. 2(b). However, the excitation near 3.8 MeV is not reproduced by the calculation. The expected exhaustion of the $E2$ sum rule for the $0\hbar\omega$ model space amounts to 16%, slightly higher than the experimental value of 11.6(8)%. The summed strength from the model is about 25% less than the experimental value. Thus from this shell model approach no significant unobserved strength is expected. We note that at energies above about 7 MeV the influence of $2\hbar\omega$ excitations might start to play a role which is not included in our model calculations.

A similarly good account of the experimental data is found from a calculation within the quasiparticle-phonon nuclear model (QPM [28]) as is shown in fig. 2(c). This calculation includes the coupling to two-particle–two-hole configurations and includes transitions over several major shells. Again, one expects a limited number of states whose strength is of the order of the detection threshold (dashed curve). The total strength up to 10 MeV in the QPM calculation amounts to 745 $e^2$fm$^4$ in good agreement

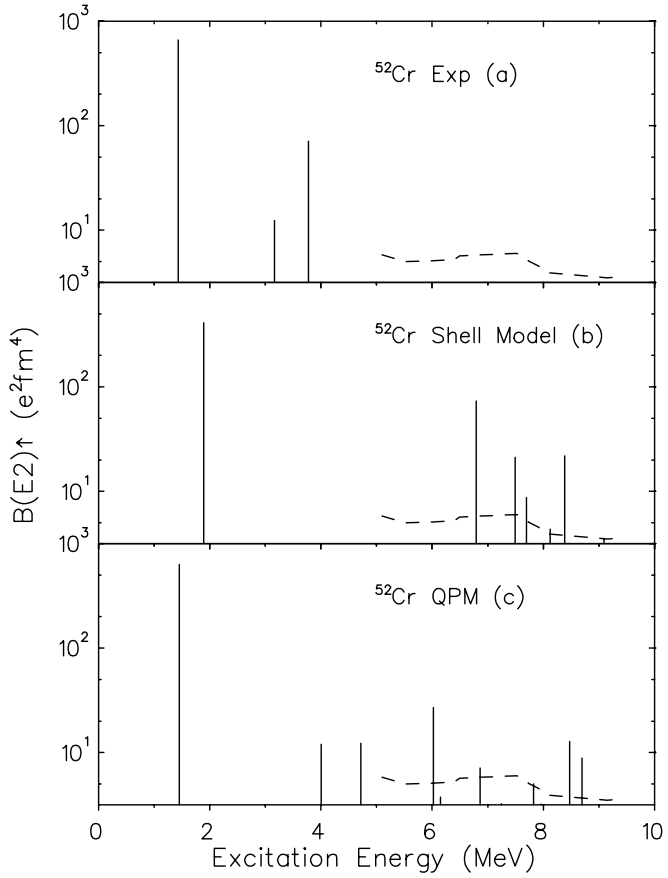


**Fig. 2.** Comparison of the $E2$ strength distributions in the semi-magic $N = 28$ nucleus $^{52}$Cr (a) as extracted from the present experiment, (b) as predicted by a $0\hbar\omega$ shell model calculation using the OXBASH code with the FPD6 interaction [26], and (c) as predicted by a quasiparticle-phonon model calculation including the coupling to two-particle–two-hole configurations. Dashed curves indicate the detection threshold for $E2$ excitations.

with the experimental data. While, as in the shell model calculation, the $E2$ strength around 4 MeV is not accurately reproduced, the energy-weighted sum in the QPM exhausts about 15% of the EWSR and thus is only little larger than the value found experimentally.

### 4.2 $^{48}$Ca

The theoretical description of the $E2$ strength distribution in $^{48}$Ca —on which we shall focus in the following— is more challenging. The experimental result of Hartmann *et al.* [5,6] is shown in panel (a) of fig. 3. A continuum-RPA approach by Kamerdzhiev and co-workers is capable of describing the observed electric dipole strength distribution up to 10 MeV [29], however, no significant $E2$ strength between 4 and 10 MeV is predicted [30,31]. We calculated the $E2$ strength distribution within the QPM, again with two-particle–two-hole configurations and including transitions over several major shells. The results are displayed in fig. 3(b) for energies up to 10 MeV and show the low-lying $E2$ strength to be concentrated in the transition to the

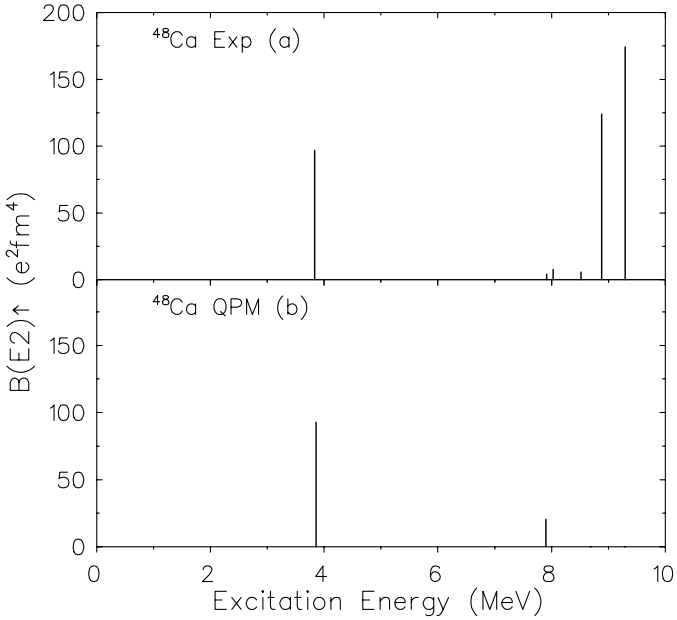


**Fig. 3.** Comparison of the $E2$ strength distributions in the doubly magic $N = 28$ nucleus $^{48}$Ca (a) as extracted from the experiment [5,6] and (b) as predicted by a quasiparticle-phonon model calculation including the coupling to two-particle–two-hole configurations.

$2_1^+$ state. The total calculated $E2$ strength up to 10 MeV is less than in the experiment, and only three additional states are predicted below 10 MeV, two of which are excited with negligible strength. To estimate the role of possible pairing effects in $^{48}$Ca we have performed an additional calculation in which the monopole pairing strength has been artificially increased to the level that the BCS calculation reproduces the measured occupation probabilities [32]. Although the number of $2^+$ states below 10 MeV is sufficiently large, no significant variation of the strength distribution is found.

An investigation of the $E2$ strength distribution within the shell model would be highly desirable for $^{48}$Ca, but only limited calculations are possible at present. Recently, an *sd*-$f_{7/2}p_{3/2}$ cross-shell interaction has been developed for the description of isotope shifts in the calcium isotopes [33]. Using this interaction with the shell model code ANTOINE [34] one finds the $E2$ strength concentrated at low energies [35], in contrast to experiment, which emphasizes the need for a universal interaction in a full *sd*-*fp* model space. Research efforts towards this goal are underway [36]. In order to reliably determine the $E2$ strength at energies beyond a few MeV, a full $2\hbar\omega$ model space should be considered.

Langanke and co-workers [37] predict for the neutron-rich nucleus $^{68}$Ni a behavior similar to the $E2$ strength distribution in $^{40,48}$Ca. Here, an accumulation of $E2$ strength is expected around 5 MeV, about 2.5 MeV above the $2_1^+$ state. The microscopic analyses presented in ref. [37] suggest that this strength distribution arises from the fact that the neutron sub-shell closure is associated with a parity change between the *fp* and *g* orbitals. A similar argument had been given by Grawe *et al.* [38], also for

**Table 2.** Compilation of summed $E2$ strengths, of the energy-weighted sums, and of the exhaustion of the energy-weighted isoscalar $E2$ sum rule up to a maximum energy of $E_{\max}$ for various magic and semi-magic nuclei. The exhaustion of the non–energy-weighted total $E2$ strength is based on the assumption that the remaining isoscalar $E2$ strength resides in the isoscalar giant quadrupole resonance located [3] at a centroid energy of $64.7\,\mathrm{MeV} \cdot A^{-1/3}$. The values for the $2_1^+$ states have been taken from the compilation of [2], and for the other $2^+$ states the ENSDF data base at the NNDC [13] has been used. The reference column lists additional photon scattering data.

| Nuclide | $E_{\max}$ (MeV) | $\sum B_i$ ($e^2\mathrm{fm}^4$) | $\sum E_{\mathrm{x},i} B_i$ ($\mathrm{MeV}\,e^2\mathrm{fm}^4$) | $\frac{\sum E_{\mathrm{x},i} B_i}{S(E2)}$ (%) | $\frac{\sum B_i}{N(E2)}$ (%) | Ref. |
|---|---|---|---|---|---|---|
| $^{16}$O | 12.0 | 61(10) | 510(100) | 28.2(56) | 54(14) | |
| $^{40}$Ca | 9.9 | 332(60) | 2096(340) | 25.1(41) | 50(14) | [5,6] |
| $^{44}$Ca | 9.9 | 473(20) | 547(23) | 6.8(3) | 53(4) | [29] |
| $^{48}$Ca | 9.9 | 407(32) | 3186(238) | 40.6(30) | 61(8) | [5,6] |
| $^{52}$Cr | 9.9 | 744(41) | 1273(92) | 11.6(8) | 57(5) | this work |
| $^{88}$Sr | 6.7 | 1114(95) | 2491(277) | 10.8(12) | 44(5) | [39] |
| $^{116}$Sn | 10.0 | 2233(79) | 3120(133) | 8.5(4) | 47(3) | [40,41] |
| $^{124}$Sn | 10.0 | 1962(85) | 2873(186) | 8.0(5) | 44(3) | [40,41] |
| $^{138}$Ba | 6.7 | 3287(245) | 6127(565) | 14.2(13) | 53(6) | [42,43] |
| $^{140}$Ce | 7.0 | 3291(90) | 5723(188) | 12.4(4) | 50(2) | [42,44] |
| $^{206}$Pb | 6.7 | 3383(235) | 10642(907) | 13.1(11) | 35(3) | [45] |
| $^{208}$Pb | 6.7 | 3838(412) | 17404(1913) | 21.5(24) | 40(6) | [45,46] |

the case of $^{68}$Ni. At the $Z = 20$, $N = 28$ shell closure the situation is similar due to the parity change between the *sd* and *fp* proton orbitals, whereas for $^{52}$Cr the relevant orbitals of both protons and neutrons are of the same parity. However, a recently published photon scattering experiment on $^{44}$Ca did not observe $E2$ strength above 4 MeV, either [29]. Thus, the picture seems to break down for semi-magic nuclei where either protons or neutrons are in an open shell.

## 5 Systematics of the E2 strengths in magic and semi-magic nuclei

### 5.1 Energy-weighted sum rule

It might be instructive to study if a large exhaustion of the isoscalar $E2$ EWSR below the ISGQR occurs in other semi-magic or magic nuclei, as well. Table 2 summarizes the extracted properties, namely the summed $E2$ strength up to the maximum energy where data are available, the energy-weighted sums up to that energy, and the EWSR exhaustion according to eq. (1). The data for the $2_1^+$ state have generally been taken from ref. [2], for the higher-lying states, information from the data base ENSDF [13] as well as from photon scattering experiments have been included. While no distinct pattern is found for the summed $B(E2)$ values (expressed in Weisskopf units and displayed in fig. 4(a)), the four doubly magic nuclei $^{16}$O, $^{40,48}$Ca, and $^{208}$Pb exhaust more than 20% of the isoscalar EWSR, on the average two times more than the other nuclei considered. This is visualized in fig. 4(b). The exhaustion of the $E2$ EWSR at energies below the ISGQR therefore might serve as a signature for a double shell closure.

The exhaustion of the $E2$ EWSR has been extracted from $\alpha$ scattering experiments at intermediate energies [47], as well. One finds, *e.g.*, for $^{16}$O an exhaustion of 25% for energies up to 14 MeV [48], in good accord with the NNDC data listed in table 2. The work by van der Borg, Harakeh, and van der Woude [49] reports an exhaustion of the $E2$ EWSR of 18(5)% for $^{40}$Ca for energies up to 12 MeV which is less than measured in photon scattering because one strong excitation at 6.91 MeV is not observed in $(\alpha, \alpha')$. Furthermore, recent results indicate that about 70%–100% of the EWSR are exhausted at energies above 10 MeV in medium-mass [50,51] and heavy nuclei [52,53] and independent of the shell structure of the investigated nuclei [51,53]. While background subtraction and data analysis may be disputed, the data show that there is not too much strength missing that could be located at low excitation energies. This sets a natural limit to possibly unobserved low-lying $E2$ strength.

### 5.2 Non–energy-weighted sum rule

It is now interesting to see if this strong exhaustion of the EWSR in doubly magic nuclei at energies well below the ISGQR also implies that the non–energy-weighted $E2$ strength dominantly resides at low energies in these nuclei. In order to get an estimate for the non–energy-weighted total $E2$ strength, where no model-independent sum rule is available, we assume that the theoretical EWSR (eq. (1)) is fully exhausted. Taking the centroid energy $E_{\mathrm{x,ISGQR}}$ of the ISGQR as extracted from experimental systematics [3], one can deduce a non–energy-weighted isoscalar $E2$ sum rule

$$N(E2) = \sum^{E_{\max}} B_i(E2)\uparrow + \frac{S(E2) - \sum^{E_{\max}} E_{\mathrm{x},i} B_i(E2)\uparrow}{E_{\mathrm{x,ISGQR}}}. \quad (2)$$

The result is depicted in fig. 4(c): the low-lying strength exhausts about 40–50% of the total isoscalar $E2$ strength

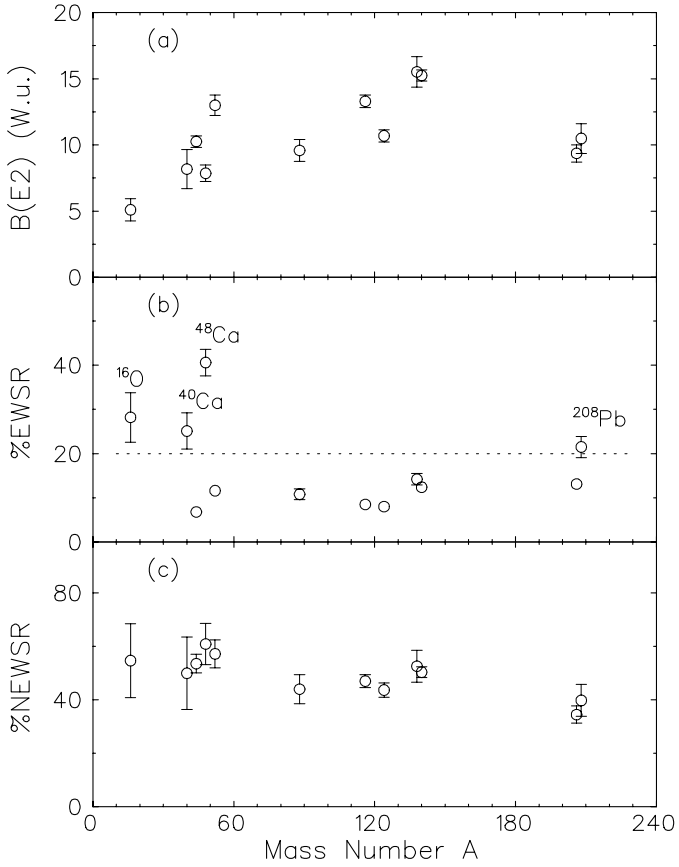


**Fig. 4.** Systematics of the summed properties of low-lying $E2$ excitations in various nuclei, cf. table 2. (a) Summed $E2$ strength located at low energies in Weisskopf units. (b) Exhaustion of the isoscalar $E2$ energy-weighted sum rule (EWSR). In the four doubly magic nuclei, $^{16}$O, $^{40,48}$Ca, and $^{208}$Pb, the low-lying states carry more than 20% of the EWSR (dotted line). (c) Exhaustion of a non–energy-weighted sum rule as obtained from the low-energy data and the centroid of the giant quadrupole resonance [3] according to eq. (2).

in all considered nuclei, independent of the individual semi- or doubly magic structure. Numerical values are given in table 2. We note, by the way, that assuming significant unobserved $E2$ strength at energies below the ISGQR in the semi-magic nuclei would consequently lead to a higher level of exhaustion of the non–energy-weighted $E2$ strength at low energies in these nuclei. Estimates like the ones discussed in sect. 3 show that more than 75% of the total strength would then reside below 10 MeV, leaving little strength for the ISGQR.

## 6 Conclusion

In summary, we have performed a photon scattering experiment on the semi-magic $^{52}$Cr nucleus, following the observation of a large exhaustion of the isoscalar $E2$ EWSR at low energies in the doubly magic $N = 28$ isotone $^{48}$Ca. While the summed $E2$ strength in $^{52}$Cr is larger than in $^{48}$Ca, the exhaustion of the $E2$ EWSR below the ISGQR is much smaller since the $E2$ strength is concentrated in the transition to the $2_1^+$ state. The existence of unobserved strength cannot be strictly excluded, but it appears unlikely from systematic arguments and model calculations. For the doubly magic $^{48}$Ca nucleus, microscopic approaches are not capable of reproducing the experimental findings. For a shell model description sophisticated cross-shell interactions in a large valence space including basically the entire *sd-fp* shells are not yet available so that present predictions are naturally of limited reliability.

A systematic survey over a wide mass range shows that a large fraction ($> 20\%$) of the isoscalar $E2$ EWSR is exhausted in doubly magic nuclei, typically two times larger than in nuclei with at least one open shell. Thus, the exhaustion of the $E2$ EWSR at low energies may serve as an experimental measure of the magicity of a nucleus. The exhaustion of the non–energy-weighted isoscalar $E2$ strength, however, is constant and hardly depends on the nuclear structure.

More theoretical and experimental efforts are needed to understand these results. Studying open-shell nuclei might be an instructive continuation of our study on closed-shell nuclei, especially as in some open-shell nuclei there is evidence for significant low-lying $E2$ strength above the first quadrupole excitation. The $\alpha$-scattering work by van der Borg, Harakeh, and van der Woude [49], *e.g.*, reports EWSR depletions of above 20% for $^{24,26}$Mg below 14 MeV. The scattering of $\alpha$-particles in comparison to photon scattering is also of particular interest for studying the isospin character of the excitations detected in photon scattering. For the electric pygmy dipole resonance, a recent $(\alpha, \alpha'\gamma)$ study by a Darmstadt-Groningen Collaboration has found a surprisingly abrupt change in the measured $\alpha$-scattering cross-sections [54] in $^{140}$Ce.

We thank H.-D. Gräf and the accelerator group at the S-DALINAC for the reliable beam during the $^{52}$Cr experiment and acknowledge the help of M. Babilon, D. Galaviz, T. Hartmann, A. Kretschmer, D. Savran, K. Vogt, and S. Volz during the experiment. Helpful discussions with B.A. Brown, K. Langanke, F. Nowacki, and A. Richter and the support of N. Ryezayeva with the OXBASH calculations are appreciated. We also thank F. Nowacki for providing us with preliminary shell model calculations using the code ANTOINE with the interaction of ref. [33]. This work has been supported by the Deutsche Forschungsgemeinschaft under contract SFB 634.

## References

1. L. Grodzins, Phys. Lett. **2**, 88 (1962).
2. S. Raman, C.W. Nestor jr., P. Tikkanen, At. Data Nucl. Data Tables **78**, 1 (2001).
3. A. van der Woude, *Electric and Magnetic Giant Resonances*, edited by J. Speth (World Scientific, Singapore, 1991) p. 99.
4. A. Shevchenko, J. Carter, R.W. Fearick, S.V. Förtsch, H. Fujita, Y. Fujita, Y. Kalmykov, D. Lacroix, J.J. Lawrie, P. von Neumann-Cosel, R. Neveling, V.Yu. Ponomarev, A. Richter, E. Sideras-Haddad, F.D. Smit, J. Wambach, Phys. Rev. Lett. **93**, 122501 (2004).

5. T. Hartmann, J. Enders, P. Mohr, K. Vogt, S. Volz, A. Zilges, Phys. Rev. Lett. **85**, 274 (2000); **86**, 4981 (2001)(E).
6. T. Hartmann, J. Enders, P. Mohr, K. Vogt, S. Volz, A. Zilges, Phys. Rev. C **65**, 034301 (2002).
7. J. Enders, P. von Brentano, J. Eberth, R.-D. Herzberg, N. Huxel, H. Lenske, P. von Neumann-Cosel, N. Nicolay, N. Pietralla, H. Prade, J. Reif, A. Richter, C. Schlegel, R. Schwengner, S. Skoda, H.G. Thomas, I. Wiedenhöver, G. Winter, A. Zilges, Nucl. Phys. A **636**, 139 (1998).
8. P. Mohr, J. Enders, T. Hartmann, H. Kaiser, D. Schiesser, S. Schmitt, S. Volz, F. Wissel, A. Zilges, Nucl. Instrum. Methods Phys. Res. A **423**, 480 (1999).
9. A. Richter, *Proceedings of the fifth European Particle Accelerator Conference, Sitges/Barcelona, 1996*, edited by S. Myers *et al.*(Institute of Physics, Bristol, 1996) p. 110.
10. R. Moreh, W.C. Sellyey, R. Vodhanel, Phys. Rev. C **22**, 1820 (1980).
11. Application Software Group, GEANT – Detector description and simulation tool, Version 3.21, CERN program library long writeup W5013 (CERN, Geneva, 1994).
12. K. Vogt, P. Mohr, M. Babilon, J. Enders, T. Hartmann, C. Hutter, T. Rauscher, S. Volz, A. Zilges, Phys. Rev. C **63**, 055802 (2001).
13. National Nuclear Data Center, Brookhaven National Laboratory, Data Base ENSDF of June 2005, `http://nndc.bnl.gov`.
14. O. Karg, Diplomarbeit, TU Darmstadt, 2004 (unpublished); O. Karg *et al.*, in preparation.
15. R.J. Peterson, Ann. Phys. (N.Y.) **53**, 40 (1969).
16. P. Demetriou, S. Goriely, Nucl. Phys. A **695**, 95 (2001).
17. `http://www.astro.ulb.ac.be/Html/bruslib.html`.
18. A. Gilbert, A.G.W. Cameron, Can. J. Phys. **43**, 1446 (1965); P.J. Brancazio, A.G.W. Cameron, Can. J. Phys. **47**, 1029 (1969).
19. W. Dilg, W. Schantl, H. Vonach, M. Uhl, Nucl. Phys. A **217**, 269 (1973).
20. T. von Egidy, D. Bucurescu, Phys. Rev. C **72**, 044311 (2005).
21. D.I. Sober, B.C. Metsch, W. Knüpfer, G. Eulenberg, G. Küchler, A. Richter, E. Spamer, W. Steffen, Phys. Rev. C **31**, 2054 (1985).
22. P. von Neumann-Cosel, A. Poves, J. Retamosa, A. Richter, Phys. Lett. B **443**, 1 (1998).
23. K. Langanke, G. Martinez-Pinedo, P. von Neumann-Cosel, A. Richter, Phys. Rev. Lett. **93**, 202501 (2004).
24. N. Kumagi, T. Ishimatsu, E. Tanaka, K. Kageyama, G. Isoyama, Nucl. Phys. A **329**, 205 (1979).
25. U.E.P. Berg, D. Rück, K. Ackermann, K. Bangert, C. Bläsing, K. Kobras, W. Naatz, R.K.M. Schneider, R. Stock, K. Wienhard, Phys. Lett. B **103**, 301 (1981).
26. W.A. Richter, M.G. van der Merwe, R.E. Julies, B.A. Brown, Nucl. Phys. A **523**, 325 (1991).
27. A. Etchegoyen, W.D. Rae, N.S. Godwin, W.A. Richter C.H. Zimmermann, B.A. Brown, W.E. Ormand, J.S. Winfield, Program OXBASH, MSU-NSCL Report 524, 1985.
28. V.G. Soloviev, *Theory of Atomic Nuclei: Quasiparticles and Phonons* (Institute of Physics, Bristol, 1992).
29. T. Hartmann, M. Babilon, S. Kamerdzhiev, E. Litvinova, D. Savran, S. Volz, A. Zilges, Phys. Rev. Lett. **93**, 192501 (2004).
30. S. Kamerdzhiev, J. Speth, G. Tertychny, Nucl. Phys. A **624**, 328 (1997).
31. S. Kamerdzhiev, J. Speth, G. Tertychny, Phys. Rep. **393**, 1 (2004).
32. Y. Uozumi, O. Iwamoto, S. Widodo, A. Nohtomi, T. Sakae, M. Matoba, M. Nakano, T. Maki, N. Koori, Nucl. Phys. A **576**, 123 (1994).
33. E. Caurier, K. Langanke, G. Martinez-Pinedo, F. Nowacki, P. Vogel, Phys. Lett. B **522**, 240 (2001).
34. E. Caurier, Program ANTOINE, CRN, Strasbourg, 1989; E. Caurier, F. Nowacki, Acta Phys. Pol. B **30**, 705 (1999).
35. F. Nowacki, private communication.
36. A.F. Lisetzkiy, E. Caurier, K. Langanke, G. Martinez-Pinedo, P. von Neumann-Cosel, F. Nowacki, A. Richter, submitted to Nucl. Phys. A.
37. K. Langanke, J. Terasaki, F. Nowacki, D.J. Dean, W. Nazarewicz, Phys. Rev. C **67**, 044314 (2003).
38. H. Grawe, M. Gorska, C. Fahlander, M. Palacz, F. Nowacki, E. Caurier, J.M. Daugas, M. Lewitowicz, M. Sawicka, R. Grzywacz, K. Rykaczewski, O. Sorlin, S. Leenhardt, F. Azaiez, Nucl. Phys. A **704**, 211c (2002).
39. L. Käubler, H. Schnare, R. Schwengner, H. Prade, F. Dönau, P. von Brentano, J. Eberth, J. Enders, A. Fitzler, C. Fransen, M. Grinberg, R.-D. Herzberg, H. Kaiser, P. von Neumann-Cosel, N. Pietralla, A. Richter, G. Rusev, Ch. Stoyanov, I. Wiedenhöver, Phys. Rev. C **70**, 064307 (2004).
40. K. Govaert, L. Govor, E. Jacobs, D. de Frenne, W. Mondelaers, K. Persyn, M.L. Yoneama, U. Kneissl, J. Margraf, H.H. Pitz, K. Huber, S. Lindenstruth, R. Stock, K. Heyde, A. Vdovin, V.Yu. Ponomarev, Phys. Lett. B **335**, 113 (1994).
41. J. Bryssinck, L. Govor, V.Yu. Ponomarev, F. Bauwens, O. Beck, D. Belic, P. von Brentano, D. De Frenne, T. Eckert, C. Fransen, K. Govaert, R.-D. Herzberg, E. Jacobs, U. Kneissl, H. Maser, A. Nord, N. Pietralla, H.H. Pitz, V. Werner, Phys. Rev. C **61**, 024309 (2000).
42. R.-D. Herzberg, I. Bauske, P. von Brentano, T. Eckert, R. Fischer, W. Geiger, U. Kneissl, J. Margraf, H. Maser, N. Pietralla, H.H. Pitz, A. Zilges, Nucl. Phys. A **592**, 211 (1995).
43. R.-D. Herzberg, C. Fransen, P. von Brentano, J. Eberth, J. Enders, A. Fitzler, L. Käubler, H. Kaiser, P. von Neumann-Cosel, N. Pietralla, V.Yu. Ponomarev, H. Prade, A. Richter, H. Schnare, R. Schwengner, S. Skoda, H.G. Thomas, H. Tiesler, D. Weisshaar, I. Wiedenhöver, Phys. Rev. C **60**, 051307(R) (1999).
44. R.-D. Herzberg, P. von Brentano, J. Eberth, J. Enders, R. Fischer, N. Huxel, T. Klemme, P. von Neumann-Cosel, N. Nicolay, N. Pietralla, V.Yu. Ponomarev, J. Reif, A. Richter, C. Schlegel, R. Schwengner, S. Skoda, H.G. Thomas, I. Wiedenhöver, G. Winter, A. Zilges, Phys. Lett. B **390**, 49 (1997).
45. J. Enders, P. von Brentano, J. Eberth, A. Fitzler, C. Fransen, R.-D. Herzberg, H. Kaiser, L. Käubler, P. von Neumann-Cosel, N. Pietralla, V.Yu. Ponomarev, A. Richter, R. Schwengner, I. Wiedenhöver, Nucl. Phys. A **724**, 243 (2003).
46. J. Enders, P. von Brentano, J. Eberth, A. Fitzler, C. Fransen, R.-D. Herzberg, H. Kaiser, L. Käubler, P. von Neumann-Cosel, N. Pietralla, V.Yu. Ponomarev, A. Richter, H. Schnare, R. Schwengner, S. Skoda, H.G. Thomas, H. Tiesler, D. Weisshaar, I. Wiedenhöver, Nucl. Phys. A **674**, 3 (2000).

47. M.N. Harakeh, A. van der Woude, *Giant Resonances – Fundamental High-Frequency Modes of Nuclear Excitation* (Oxford University Press, Oxford, New York, 2001).
48. M.N. Harakeh, A.R. Arends, M.J.A. de Voigt, A.G. Drentje, S.Y. van der Werf, A. van der Woude, Nucl. Phys. A **265**, 189 (1976).
49. K. van der Borg, M.N. Harakeh, A. van der Woude, Nucl. Phys. A **365**, 243 (1981).
50. D.H. Youngblood, Y.-W. Lui, H.L. Clark, Phys. Rev. C **63**, 067301 (2001); **64**, 049901 (2001)(E).
51. Y.-W. Lui, D.H. Youngblood, H.L. Clark, Y. Tokimoto, B. John, Phys. Rev. C **73**, 014314 (2006).
52. Y.-W. Lui, D.H. Youngblood, Y. Tokimoto, H.L. Clark, B. John, Phys. Rev. C **70**, 014307 (2004).
53. D.H. Youngblood, Y.-W. Lui, H.L. Clark, B. John, Y. Tokimoto, X. Chen, Phys. Rev. C **69**, 034315 (2004).
54. D. Savran, M. Babilon, A.M. van den Berg, M.N. Harakeh, J. Hasper, A. Matic, H.J. Wörtche, A. Zilges, Phys. Rev. Lett. **97**, 172502 (2006).